International Journal of Legal Medicine (2023) 137:875–886
https://doi.org/10.1007/s00414-023-02971-w

ORIGINAL ARTICLE

Detection of multiple biomarkers associated with satellite cell fate in the contused skeletal muscle of rats for wound age estimation

Zhi-Ling Tian[1] · Ruo-Lin Wang[2,3] · Qi-Fan Yang[1] · Zhi-Qiang Qin[1] · He-Wen Dong[1] · Dong-Hua Zou[1] · Zheng-Dong Li[1] · Jin-Ming Wang[1] · Da-Wei Guan[4] · Jian-Hua Zhang[1] · Ning-Guo Liu[1]

Received: 12 May 2022 / Accepted: 8 February 2023 / Published online: 17 February 2023

Abstract

From the perspective of forensic wound age estimation, experiments related to skeletal muscle regeneration after injury have rarely been reported. Here, we examined the time-dependent expression patterns of multiple biomarkers associated with satellite cell fate, including the transcription factor paired box 7 (Pax7), myoblast determination protein (MyoD), myogenin, and insulin-like growth factor (IGF-1), using immunohistochemistry, western blotting, and quantitative real-time PCR in contused skeletal muscle. An animal model of skeletal muscle contusion was established in 30 Sprague–Dawley male rats, and another five rats were employed as non-contused controls. Morphometrically, the data obtained from the numbers of Pax7 + , MyoD + , and myogenin + cells were highly correlated with the wound age. Pax7, MyoD, myogenin, and IGF-1 expression patterns were upregulated after injury at both the mRNA and protein levels. Pax7, MyoD, and myogenin protein expression levels confirmed the results of the morphometrical analysis. Additionally, the relative quantity of IGF-1 protein > 0.92 suggested a wound age of 3 to 7 days. The relative quantity of *Pax7* mRNA > 2.44 also suggested a wound age of 3 to 7 days. Relative quantities of *Myod1*, *Myog*, and *Igf1* mRNA expression > 2.78, > 7.80, or > 3.13, respectively, indicated a wound age of approximately 3 days. In conclusion, the expression levels of Pax7, MyoD, myogenin, and IGF-1 were upregulated in a time-dependent manner during skeletal muscle wound healing, suggesting the potential for using them as candidate biomarkers for wound age estimation in skeletal muscle.

Keywords Wound age estimation · Skeletal muscle contusion · Muscle regeneration · Satellite cell fate · Forensic pathology

Introduction

Wound age estimation is an extremely important issue in forensic pathology because it can provide valuable medical information for criminal identification [1, 2]. Wound age has typically been assessed using diverse techniques and methods for searching for chronological biomarkers, consisting of the appearance of effector cells and expression of regulatory mediators (cytokines, growth factors, and others) in the process of wound healing [3–9]. In the past decades, forensic pathologists have performed extensive research on wound age estimation by examining inflicted wounds in common tissues such as the skin, skeletal muscle, and brain. This has provided useful information and vital experimental data for estimating wound age in forensic practice [9–14]. However, studies regarding muscle regeneration after injury are rarely reported from the perspective of forensic wound age estimation [15].

Skeletal muscles possess a remarkable ability to regenerate in response to injury. Muscle regeneration is a complicated but well-coordinated process, in which a variety of cellular and molecular events are involved [16, 17]. This process mainly depends on satellite cells (SCs) which are mitotically quiescent under normal physiological conditions and comprise approximately 1 to 4% of muscle nuclei in adult skeletal muscle. Upon muscle injury, SCs become activated, proliferate extensively, undergo differentiation into myocytes, and fuse with each other or damaged

Zhi-Ling Tian and Ruo-Lin Wang contributed equally to this article.

✉ Da-Wei Guan
dwguan@mail.cmu.edu.cn

✉ Jian-Hua Zhang
Zhangjh@ssfjd.cn

✉ Ning-Guo Liu
Liung@ssfjd.cn; liuningguo@foxmail.com

Extended author information available on the last page of the article

myofibers to repair injured muscle [18, 19]. The behavior and fate of SC populations during muscle regeneration are regulated by multiple factors, such as the transcription factor paired box 7 (Pax7), myoblast determination protein (MyoD), and myogenin, as well as inflammatory reactions and more [20, 21]. Substantial evidence demonstrates that Pax7 is a classical marker for SCs in the quiescent/activated myogenic state, MyoD is the marker for SCs in proliferated/differentiated state, and myogenin is the marker for terminally differentiated [22–26]. Additionally, insulin-like growth factor (IGF-1) contributes significantly to muscle regeneration after injury by promoting the proliferation and differentiation of SCs [27]. From the abovementioned findings, we speculated that the dynamics of Pax7, MyoD, myogenin, and IGF-1 may be closely related to wound age during muscle regeneration after injury.

It is widely believed that combined detection and analysis of morphological and molecular biological parameters can reduce error margins in wound time calculations [12, 28]. In the present study, we investigated the dynamics of Pax7, MyoD, myogenin, and IGF-1 by immunohistochemistry (IHC), western blotting, and quantitative real-time PCR (qPCR) during skeletal muscle regeneration in a contusion model of rats, aiming to provide fundamental data and preliminary insight for estimating wound age.

Materials and methods

Animal model of skeletal muscle contusion

All animal protocols conformed to the "Principles of Laboratory Animal Care" (National Institutes of Health Publication No. 85–23, revised 1985) to minimize both the number of animals used in a procedure and any suffering that they might experience. All protocols were performed according to the Guidelines for the Care and Use of Laboratory Animals of China Medical University.

A reproducible muscle contusion model in rats was described previously [9, 15]. A total of 35 adult Sprague–Dawley male rats weighing 300 to 320 g were used in our study. Briefly, 30 rats were anesthetized by intraperitoneal injection with 2% sodium pentobarbital (30 mg/kg). The right hindlimb was positioned on a board in a prone position by extending the knee and dorsiflexing the ankle to 90°. A single impact at a velocity of 3 m/s was delivered to the gastrocnemius and soleus of the right posterior limb. The size of impact interface of the counterpoise (weighing 500 g) was 1.127 cm^2. After injury, each rat was housed individually and kept under a 12-h light–dark cycle. Rats were fed with commercial rat chow and water ad libitum. All rats were sacrificed by intraperitoneal injection of a lethal dose of pentobarbital (350 mg/kg) at 1, 3, 5, 7, 9, and 14 days post-trauma (five rats at each posttraumatic interval). Gastrocnemius was taken and equally divided into two blocks. One block was used for morphological evaluation, and another was used for molecular biology assays. For the five control rats, gastrocnemius was harvested after anesthetization with an overdose of pentobarbital. No bone fracture was detected at dissection.

Antibodies

The following monoclonal antibodies (mAbs) or polyclonal antibodies (pAbs) were commercially obtained: mouse anti-Pax7 mAb (sc-365613, Santa Cruz Biotechnology, Dallas, TX, USA), mouse anti-MyoD mAb (sc-71629, Santa Cruz Biotechnology), mouse anti-myogenin mAb (sc-12732, Santa Cruz Biotechnology), rabbit anti-IGF-1 pAb (20,214–1-AP, Proteintech Group, Chicago, IL, USA), rabbit anti-GAPDH pAb (ab37168, Abcam, Cambridge, UK), horseradish peroxidase (HRP)–conjugated goat anti-mouse IgG (sc-2005, Santa Cruz Biotechnology), and biotinylated donkey anti-rabbit IgG (ab6801, Abcam).

Tissue preparation and morphometric analysis

The skeletal muscle specimens were fixed in 4% paraformaldehyde with phosphate-buffered saline (PBS, pH 7.4) and embedded in paraffin. Serial 5-μm-thick sections were prepared. IHC staining was performed using the streptavidin-peroxidase method, detecting the SCs at different myogenic states with the Pax7, MyoD, and myogenin biomarkers. Briefly, deparaffinized sections were heated for 5 min in 0.01 mol/L sodium citrate buffer (pH 6.0) for antigen retrieval. Endogenous peroxidase activity was quenched with 3% hydrogen peroxide and non-specific binding was blocked with 10% non-immune goat serum. Thereafter, the sections were incubated with mouse anti-Pax7 mAb (dilution 1:200), anti-MyoD mAb (dilution 1:100), or anti-myogenin mAb (dilution 1:200) overnight at 4 °C, followed by incubation with the corresponding Histostain-Plus Kit (Zymed Laboratories, South San Francisco, CA, USA) according to the manufacturer's instructions. Normal mouse IgG or PBS was used in place of the primary antibodies as a negative control. The sections were routinely counterstained with hematoxylin. In addition, hematoxylin–eosin (H&E) staining was conventionally conducted as in our previous study [15, 29].

For positive-cell number evaluation, 10 microscopic fields were randomly selected at 400-fold magnification in the injured area in each section. Pax7+, MyoD+, and myogenin+cell numbers were calculated in each microscopic field, and the average number of the 10 selected microscopic fields was evaluated in each wound specimen. All measurements and data analysis were performed independently by two forensic pathologists.

Protein preparation and immunoblotting assay

The skeletal muscle samples were ground into powder with liquid nitrogen using a grinder and homogenized with a sonicator in RIPA buffer (sc-24948, Santa Cruz Biotechnology) containing protease inhibitors at 4 °C. As described previously [15], homogenates were centrifuged and the resulting supernatants were collected, then protein concentrations were quantified using the bicinchoninic acid method. For immunoblotting analysis, 30 μg of protein samples was separated on a sodium dodecyl sulfate-polyacrylamide electrophoresis (SDS-PAGE) gel and transferred onto PVDF membranes (Millipore, Billerica, MA, USA). After being blocked with 5% non-fat dry milk in Tris-buffered saline-Tween-20 at room temperature (RT) for 2 h, the membranes were incubated with mouse anti-Pax7 pAb (dilution 1:200), mouse anti-MyoD mAb (dilution 1:200), mouse anti-myogenin mAb (dilution 1:200), or rabbit anti-IGF-1 (dilution 1:1000) at 4 °C overnight. Moreover, rabbit anti-GAPDH pAb (dilution 1:1000) was used for relative protein quantitation. After incubation at RT for 2 h with HRP-conjugated secondary antibody, the blots were visualized with western blotting luminol reagent (sc-2048, Santa Cruz Biotechnology) by the Electrophoresis Gel Imaging Analysis System (MF-ChemiBIS 3.2, DNR Bio-Imaging Systems, ISR). Subsequently, densitometric analyses of the bands were semi-quantitatively conducted using Scion Image software (Scion Corporation, MD, USA).

Total RNA extraction and quantitative qPCR

Total RNA was extracted from the skeletal muscle specimens with RNAiso Plus (9108, Takara Biotechnology, Shiga, Japan) according to the manufacturer's instructions. Optical density (OD) values of each RNA sample were measured using an ultraviolet spectrophotometer. A260/A280 values ranged from 1.8 to 2.0. Subsequently, 250 ng of RNA was reverse transcribed into cDNA in a 20 μL reaction volume using the PrimeScript™ RT reagent Kit (RR037A, Takara Biotechnology). The resulting cDNA was used for qPCR to quantify mRNA expression levels of *Pax7*, *Myod1*, *Myog*, and *Igf1*, with *Gapdh* as an internal control. The specific sequences of these primers are shown in Table 1. qPCR amplification was performed with an Applied Biosystems 7500 Real-Time PCR System using the SYBR® PrimeScript™ RT-PCR Kit (RR081A, Takara Biotechnology). To exclude any potential contamination, negative controls were also performed with ddH_2O instead of cDNA during each run. No amplification product was detected. The qPCR procedure was repeated at least three times for each sample.

Statistical analysis

Data are expressed as mean ± standard deviation (SD) and analyzed using PRISM 8.0 software. A one-way ANOVA was used for data analysis between two groups. Differences with $p < 0.05$ were considered to be statistically significant.

Results

Histological examination

In sections stained with H&E, hemorrhage, edema, and degeneration were observed in the contused skeletal muscles. A number of polymorphonulcear cells (PMNs) appeared in wound zones at 1 day post-wounding (Fig. 1b). At 3 days post-wounding, a large number of long spindle-shaped cells and round-shaped mononuclear cells (MNCs) were observed in the wound zones (Fig. 1c). From 5 to 9 days post-wounding, a large number of fibroblastic cells (FBCs), concomitant with regenerated multinucleated myotubes, were observed in the wounds (Fig. 1d, e). At

Table 1 Real-time PCR primer sequences

Gene	GenBank accession	Primer	Product size (bp)
Pax7	NM_ 001,191,984.1	Forward: 5′-GAT TAG CCG AGT GCT CAG AAT CAA G-3′	166
		Reverse: 5′-GTC GGG TTC TGA TTC CAC GTC-3′	
Myod1	NM_176079.1	Forward: 5′-AAT CCG ATT TAC CAG GTG CTC-3′	147
		Reverse: 5′-GGC TTT GAA AGG ACA ATT GGG-3′	
Myog	NM_ 017,115.2	Forward:5′-AGT GCC ATC CAG TAC ATT GAG-3′	127
		Reverse: 5′-TGT GGG AGT TGC ATT CAC TG-3′	
Igf1	NM_ 178,866.2	Forward:5′-AAA GTC AGC TCG TTC CAT CC-3′	149
		Reverse: 5′-GTG GCA TTT TCT GTT CCT CG-3′	
Gapdh	NM_017008.4	Forward: 5′-CAT CTC CCT CAC AAT TCC ATC C-3′	100
		Reverse: 5′-GAG GGT GCA GCG AAC TTT AT -3′	

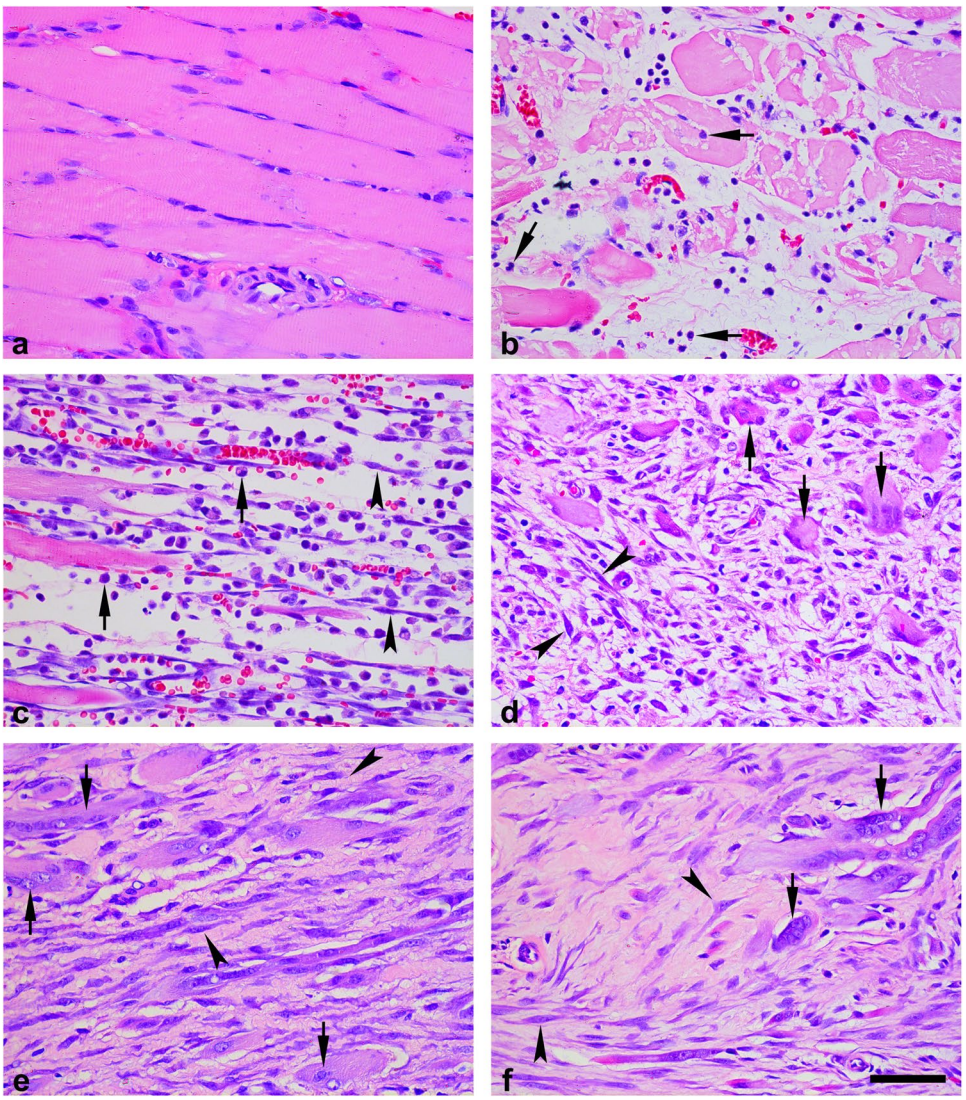

Fig. 1 H&E staining in rat skeletal muscle samples. **a** Normal skeletal muscles as a control. **b** PMNs are detected at 1 day after contusion (arrows). **c** Round-shaped MNCs (arrows) and long spindle-shaped cells (arrowheads) are present in the injured tissue at 3 days after contusion. **d**, **e** FBCs (arrowheads) concomitant with regenerated multinucleated myotubes (arrows) are observed in the areas of contusion at 5 and 9 days after contusion. **f** Some FBCs (arrowheads), fibrotic tissue, and regenerated multinucleated myotubes (arrows) were detectable in the wound zones at 14 days after injury. Scale bar, 50 μm

14 days post-wounding, some fibroblastic cells, fibrotic tissue, and regenerated multinucleated myotubes were detectable (Fig. 1f).

IHC examination and morphometric analysis

In the regeneration process after contusion, Pax7 + (SCs in the quiescent/activated state), MyoD + (SCs in the proliferated/differentiated state), and myogenin + (SCs in the differentiated state/regenerated multinucleated myotubes) cells were observed and analyzed, and their immunoreactivities were all detected in the nucleus (Fig. 2).

In control skeletal muscle specimens, only a few Pax7 + cells were observed. The number of Pax7 + cells increased significantly from 3 days, peaked at 5 days after injury, and decreased gradually in the following days. Numerous Pax7 + cells were detected near the regenerated myotubes at wound zones from 5 days post-wounding (Figs. 2a and. 3a). Statistically, the average number of Pax7 + cells was > 20 from 3 to 7 days ($p = 0.003$) and > 35 at 5 days (42.10 ± 6.06, $p = 0.002$) after injury (Fig. 3a, Table 2). The average number of Pax7 + cells was significantly lower at 1 day (7.40 ± 2.41) compared to other posttraumatic intervals, which was < 10 ($p = 0.015$; Fig. 3a, Table 2). Although there was no statistical difference between the number of Pax7 + cells at 3 and 7 days post-wounding, the two posttraumatic intervals can be distinguished by the presence or absence of regenerated myotubes.

In the control specimens, no MyoD + cell was detected. In the wounded samples, MyoD + cells emerged at 1 day, and increased dramatically at 3 days post-wounding when the positive cells presented as bead-like patterns. At 5 days post-wounding, lots of MyoD + cells were observed as the newly formed multinucleated myotubes. From 7 days post-wounding, the intensity for MyoD immunoreactivity signals in the myotubes began to wane and the positive cells gradually decreased in number with the extension

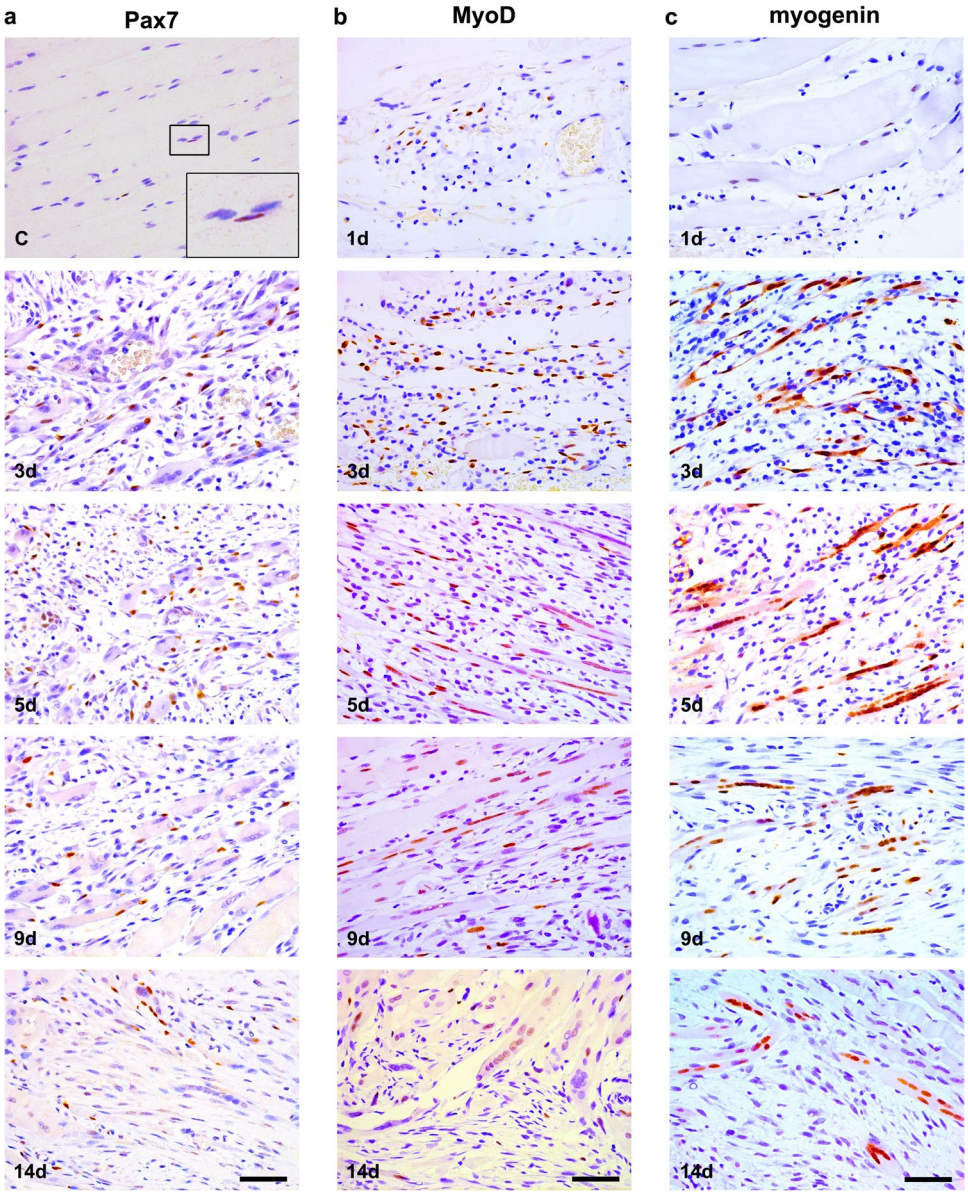

Fig. 2 IHC staining results in rat skeletal muscle samples. **a** Representative IHC staining results of Pax7 at different posttraumatic intervals, and **C** represents the result obtained from the normal skeletal muscle as a control. **b** Representative IHC staining results of MyoD at different posttraumatic intervals. **c** Representative IHC staining results of myogenin at different posttraumatic intervals. Pax7, MyoD and myogenin immunoreactivities were all detected in the nucleus. Scale bar, 50 μm

of posttraumatic interval (Figs. 2b and 3b). The average number of MyoD + cells was > 50 at 3 days (64.50 ± 6.13, $p < 0.001$) and 5 days (70.60 ± 6.65, $p < 0.001$) post-wounding, which was significantly more than that at other posttraumatic intervals. Moreover, the average number of MyoD + cells was significantly lower at 1 day (7.30 eover, compared to other posttraumatic intervals, which was < 10 ($p < 0.001$; Fig. 3b, Table 2).

There was no myogenin + cell detected in the control specimens. In the wounded samples, the myogenin + cells showed similar immunoreactivity as the aforementioned MyoD + cells from 1 to 3 days post-wounding. From 5 to 9 days post-wounding, numerous myogenin + cells were observed as the regenerated multinucleated myotubes. At 14 days post-wounding, the myogenin + cells clearly decreased in number with weakened immunoreactivity signals for myogenin (Figs. 2c and 3c). Morphometrically, the average number of myogenin + cells was > 50 from 3 to 9 days post-wounding ($p < 0.05$; Figs. 3c and 4c, Table 2), which was significantly more than that at other posttraumatic intervals. In addition, the average number of myogenin + cells at 1 day (< 10, $p = 0.008$) was lower significantly than other posttraumatic intervals. And the average number of myogenin + cells was > 30 and < 50 at 14 days after injury ($p = 0.01$; Fig. 3c, Table 2).

The ratios of MyoD + to Pax7 + cells, myogenin + to Pax7 + cells, and myogenin + to MyoD + cells in number at different posttraumatic intervals were analyzed and are shown in Fig. 3d–f. Statistically, the ratio of MyoD + to Pax7 + cells number from 3 to 14 days post-wounding was significantly higher than that at 1 day (< 1.50, $p = 0.025$).

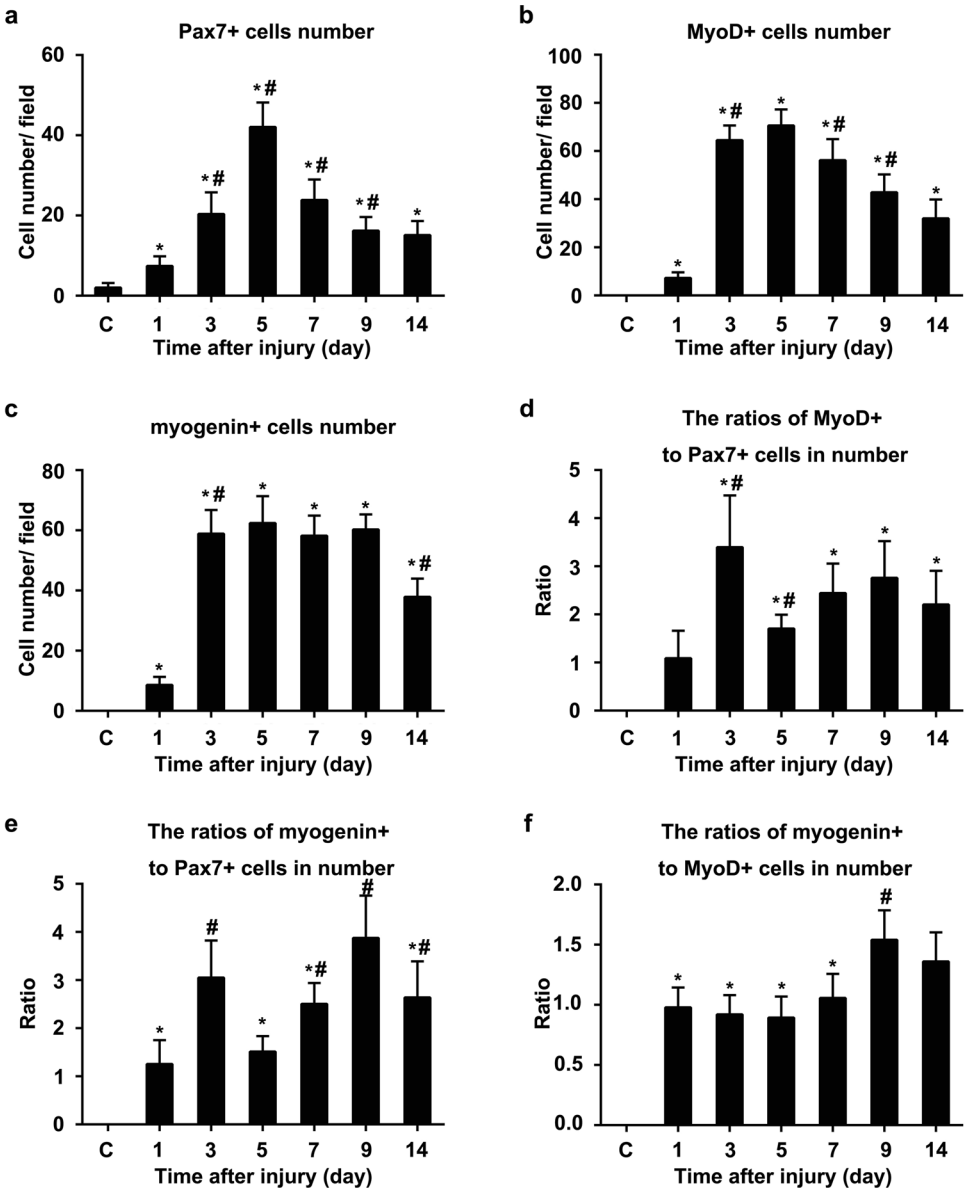

Fig. 3 Statistical analysis results of the positive-cell numbers and ratios in immunohistochemistry. All data were presented as mean ± SD and analyzed using one-way ANOVA. **a**, **b**, **c** $^{*}p < 0.05$ (vs control group), $^{\#}p < 0.05$ (vs preceding posttraumatic group). **d** $^{*}p < 0.05$ (vs 1 day group post-injury), $^{\#}p < 0.05$ (vs preceding posttraumatic group). **e** $^{*}p < 0.05$ (vs 9 days group post-injury), $^{\#}p < 0.05$ (vs 1 day group post-injury). **f** $^{*}p < 0.05$ (vs 14 days group post-injury), $^{\#}p < 0.05$ (vs preceding posttraumatic group)

Table 2 The average number of Pax7 +, MyoD +, and myogenin + cells at different posttraumatic intervals

Time after injury (day)	Cell number (mean ± SD)		
	Pax7 + cells	MyoD + cells	myogenin + cells
C	2.00 ± 1.15	0	0
1	7.40 ± 2.41*	7.30 ± 2.31*	8.60 ± 2.71*
3	20.40 ± 5.40*#	64.50 ± 6.13*#	58.90 ± 7.85*#
5	42.10 ± 6.06*#	70.60 ± 6.65*	62.40 ± 8.97*
7	23.90 ± 5.08*#	56.20 ± 8.74*#	58.20 ± 6.68*
9	16.20 ± 3.42*#	42.90 ± 7.37*#	60.30 ± 4.99*
14	15.10 ± 3.54*	32.00 ± 7.84*	37.90 ± 6.04*#

C represents the normal skeletal muscle as a control

$^{*}p < 0.05$ (vs control group), $^{\#}p < 0.05$ (vs preceding posttraumatic group)

The ratio of myogenin + to Pax7 + cells number was > 3.88 at 9 days post-wounding, which was statistically significant as compared with other posttraumatic intervals except that at 3 days post-wounding ($p = 0.028$). The ratio of myogenin + to MyoD + cells number at 9 or 14 days post-wounding was significantly higher than those of other posttraumatic intervals, which were > 1.36 ($p = 0.038$).

The cell numbers and ratios in relation to wound age are summarized in Table 3.

Western blotting and qPCR

The blots using Pax7, MyoD, myogenin, IGF-1, and GAPDH antibodies are shown in Fig. 4a. The relative quantity of Pax7 protein was significantly increased at

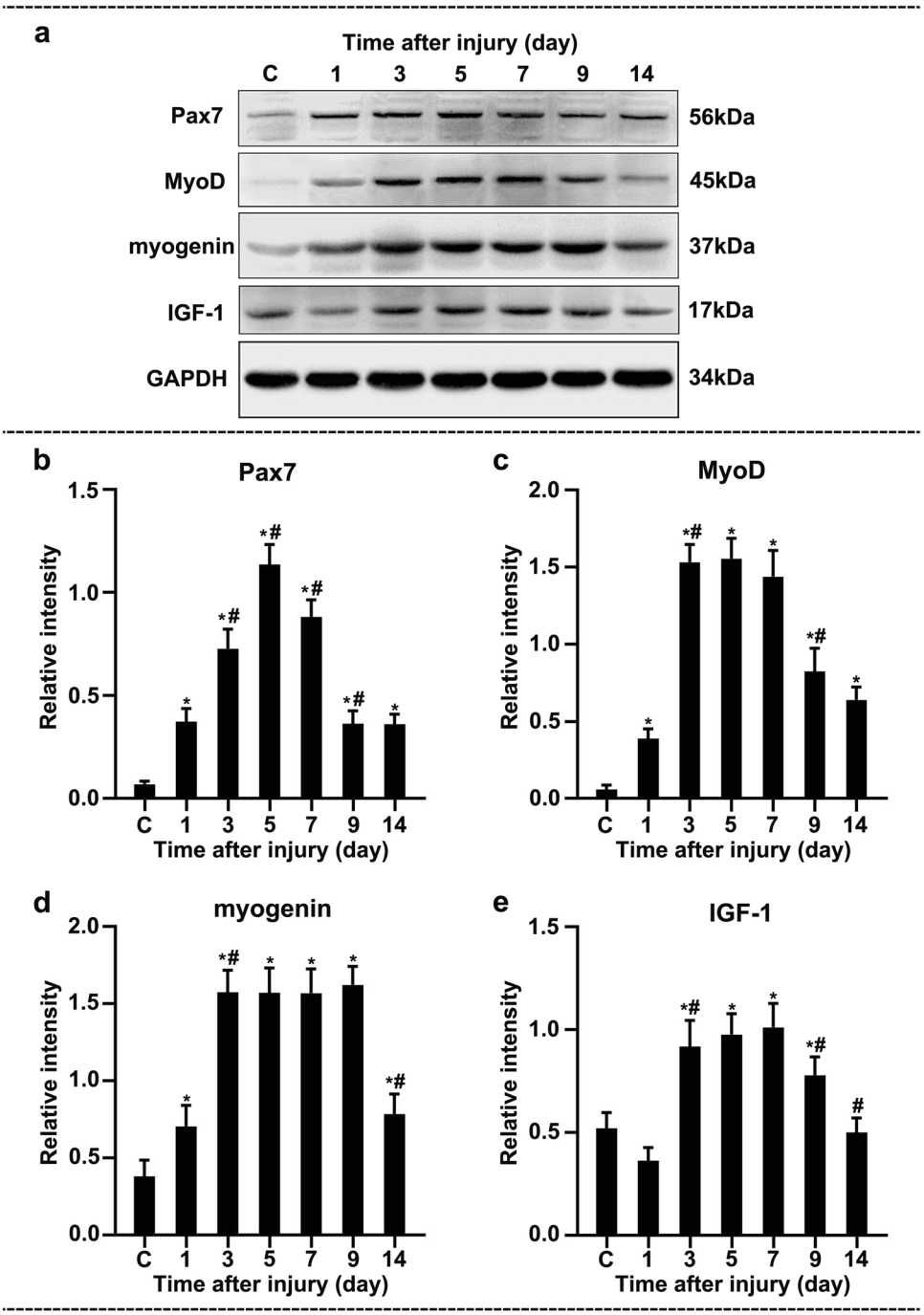

Fig. 4 Western blotting assays. **a** Representative immunoblotting results of Pax7, MyoD, myogenin, IGF-1, and GAPDH at different posttraumatic intervals in rat skeletal muscle specimens, the molecular weight of each band is indicated. *Lane C* represents the result of the control skeletal muscle sample. **b** Relative intensity of Pax7 to GAPDH. **c** Relative intensity of MyoD to GAPDH. **d** Relative intensity of myogenin to GAPDH. **e** Relative intensity of IGF-1 to GAPDH. All values are expressed as the mean ± SD (n = 5). $^{*}p < 0.05$ (vs control group), $^{\#}p < 0.05$ (vs preceding posttraumatic group)

1 day post-injury and peaked at 5 days post-injury (> 1.13, $p < 0.001$), then gradually decreased in the following days (Fig. 4b). The relative quantity of MyoD protein was > 1.40 from 3 to 7 days post-injury ($p = 0.025$), which was significantly higher than that of the other posttraumatic interval (Fig. 4c). The relative quantity of myogenin protein was at the highest level from 3 to 9 days post-injury (> 1.57, $p = 0.006$), then descended rapidly at 14 days post-injury (Fig. 4d). The relative quantity of IGF-1 protein increased dramatically at 3 days post-injury and remained at its highest level from 3 to 7 days post-injury (> 0.92, $p = 0.038$), then decreased thereafter and normalized at 14 days post-injury (Fig. 4e). Additionally, significant differences in the relative expression levels of Pax7, MyoD, and myogenin proteins were all noted from 1 to 14 days post-injury, as compared with that of control ($p < 0.05$, Fig. 4b–d).

The time-dependent mRNA expression levels of the target genes (*Pax7*, *Myod1*, *Myog*, and *Igf1*) are shown in Fig. 5. The relative quantity of *Pax7* mRNA expression increased dramatically at 3 days post-injury, remained at its highest

Table 3 Results in relation to wound age

Methods	Biomarkers		Time after injury (day)					
			1	3	5	7	9	14
Morphometric analysis	Cells number	Pax7 +	< 10 ↑	> 20 ↑	> 35 ↑	> 20 ↑	↑	↑
		MyoD +	< 10 ↑	> 50 ↑	> 50 ↑	↑	↑	↑
		myogenin +	< 10 ↑	> 50 ↑	> 50 ↑	> 50 ↑	> 50 ↑	> 30, < 50 ↑
	The presence or absence of regenerated myotubes		Absence	Absence	Presence	Presence	Presence	Presence
	Ratios	B/A	< 1.50					
		C/A		> 3.88			> 3.88	
		C/B					> 1.36	> 1.36
Western blotting	Pax7		↑	↑	> 1.13 ↑	↑	↑	↑
	MyoD		↑	> 1.40 ↑	> 1.40 ↑	> 1.40 ↑	↑	↑
	Myogenin		↑	> 1.57 ↑	> 1.57 ↑	> 1.57 ↑	> 1.57 ↑	↑
	IGF-1		——	> 0.92 ↑	> 0.92 ↑	> 0.92 ↑	↑	——
qPCR	*Pax7*		——	> 2.44 ↑	> 2.44 ↑	> 2.44 ↑	↑	——
	Myod1		↑	> 2.78 ↑	↑	↑	——	——
	Myog		↑	> 7.80 ↑	↑	↑	↑	——
	Igf1		——	> 3.13 ↑	↑	——	——	——

A: the average number of Pax7 + cells; B: the average number of MyoD + cells; C: the average number of myogenin + cells

—— represents no significant difference compared with the control

↑ represents significantly increase compared with the control

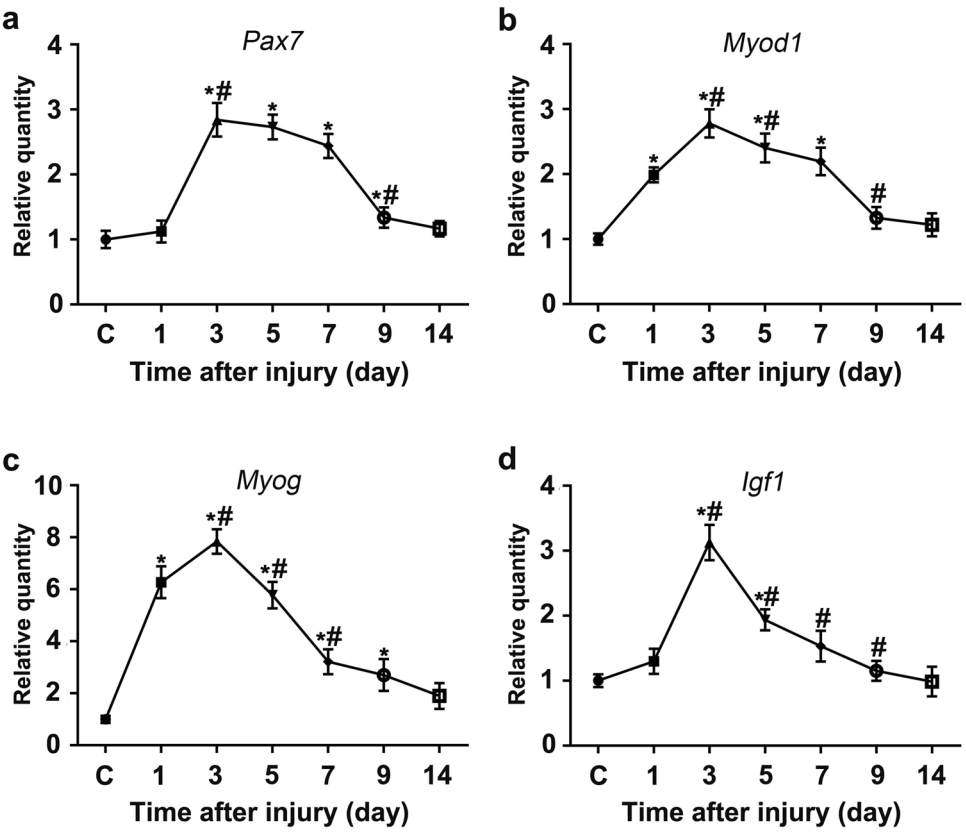

Fig. 5 qPCR assays from rat skeletal muscle specimens. **a** Relative quantity of *Pax7* mRNA expression. **b** Relative quantity of *Myod1* mRNA expression. **c** Relative quantity of *Myog* mRNA expression. **d** Relative quantity of *Igf1* mRNA expression. All values are expressed as the mean ± SD ($n = 5$). $^{*}p < 0.05$(vs control group), $^{\#}p < 0.05$ (vs preceding posttraumatic group)

level from 3 to 7 days post-injury (> 2.44, $p = 0.001$), and decreased in the following days (Fig. 5a). The relative quantities of *Myod1* and *Myog* mRNA expression were both significantly increased at 1 day post-injury and peaked at 3 days after injury at > 2.78 ($p = 0.04$) and > 7.80 ($p = 0.003$), respectively. The levels gradually decreased thereafter (Fig. 5b–c). Compared with that in the control specimens, the relative quantity of *Igf1* mRNA expression was significantly increased from 3 to 5 days post-injury ($p < 0.05$) and peaked at 3 days (> 3.13, $p = 0.002$) post-injury (Fig. 5d). In addition, significant differences in the relative quantities of *Pax7*, *Myod1*, and *Myog* mRNA expression were observed respectively from 3 to 9 days ($p = 0.03$), from 1 to 7 days ($p < 0.001$), and from 1 to 9 days ($p = 0.02$) post-injury, as compared with that of control (Fig. 5a–c).

The assays of Pax7, MyoD, myogenin, and IGF-1 by western blotting and qPCR in relation to wound age were summarized in Table 3.

Discussion

SCs are the primary population of adult skeletal muscle stem cells. Upon muscle injury, quiescent SCs become activated, proliferate, and sequentially differentiate to promote muscle regeneration [18, 19]. Pax7 is a transcription factor from the paired box family of proteins, which maintains SC survival or proliferation and prevents precociously myogenic differentiation [25, 30]. Both MyoD and myogenin belong to the myogenic regulatory factor family and contain a helix-loop-helix motif. After trauma to muscle, MyoD expression is rapidly initiated during the SC cycle, followed by myogenin expression [17]. MyoD initiates SC proliferation and subsequently signals the initiation of differentiation by cell cycle arrest. Myogenin expression is closely involved in SC differentiation and myotube formation [20, 31]. IGF-1 can be synthesized and secreted by nerve cells, capillaries, and SCs in different myogenic states and myotubes during skeletal muscle wound repair, which promotes SC proliferation and differentiation and inhibits inflammation [32–34]. Taken together, Pax7, MyoD, myogenin, and IGF-1 play corresponding and critical roles for SC fate determination that range from activation, proliferation, and differentiation to the regenerated myotubes after muscle injury. Our previous study preliminarily demonstrated that Pax7 and MyoD were upregulated in a time-dependent manner after skeletal muscle contusion [15]. In this fundamental study, we further detected the dynamics of multiple biomarkers associated with SC fate in the contused skeletal muscle of rats, including Pax7, MyoD, myogenin, and IGF-1, and found them discriminative parameters for wound age estimation.

IHC detection of specific cells or molecules that can contribute to wound age estimation has been widely employed in the forensic pathology research field [35–40]. SCs in the quiescent/activated or proliferated/differentiated states are marked using Pax7 and MyoD, respectively, and myogenin can mark the differentiated SCs and regenerated multinucleated myotubes [22, 23, 25]. Thus, we attempted to estimate wound age by morphometrical analysis in this study. The ratios of MyoD + to Pax7 + cells, myogenin + to Pax7 + cells, or myogenin + to MyoD + cells in number indirectly reflected the relative progress of the muscle regeneration. As shown in Table 3, the combined analysis of the average number of Pax7 +, MyoD +, and myogenin + cells, the abovementioned ratios, and the presence or absence of regenerated myotubes could provide significant chronological information. We observed the following: (1) the average number of Pax7 +, MyoD +, or myogenin + cells < 10 or the ratio of MyoD + to Pax7 + cells in number < 1.5 indicated that the wound age was approximately 1 day; (2) the average number of Pax7 + cells > 20, the average number of MyoD + and myogenin + cells > 50, and the ratio of myogenin + to Pax7 + cells in number > 3.88 indicated that the wound age was approximately 3 days; (3) the average number of Pax7 + cells > 35 may be a parameter for a wound age of 5 days; (4) the presence of regenerated myotubes, the ratio of myogenin + to Pax7 + cells in number > 3.88, and the ratio of myogenin + to MyoD + cells in number > 1.36 indicated that the wound age was approximately 9 days; (5) the average number of myogenin + cells being between 30 and 50, the presence of regenerated myotubes, and the ratio of myogenin + to MyoD + cells in number > 1.36 indicated that the wound age was approximately 14 days.

Recently, western blotting and qPCR have also been widely applied in the forensic wound age estimation research field because of their accuracy and sensitivity for detecting biological markers [2, 9, 13, 35, 41–43]. Moreover, combined detection of protein and mRNA may be more stable and sensitive than morphometrical assays alone for estimating wound age [28, 35]. Therefore, we further investigated the expression levels of Pax7, MyoD, myogenin, and IGF-1 using western blotting and qPCR, then attempted to estimate wound age using the data from these two techniques. The patterns of Pax7, MyoD, and myogenin protein expression were nearly consistent with the results of the morphometrical analysis. Additionally, the relative quantity of IGF-1 protein remained at its highest level from 3 to 7 days post-injury when numerous SCs in the proliferated and differentiated states were also observed (Figs. 2, 3, and 4), implying that IGF-1 contributes to SC proliferation and differentiation [33, 34]. The relative quantity of *Pax7* mRNA > 2.44 suggests a wound age of 3 to 7 days. The relative quantities of

Myod1, *Myog*, and *Igf1* mRNA all peaked at 3 days post-injury, which were respectively > 2.78, > 7.80, and > 3.13, suggesting a wound age of 3 days.

In this study, we further listed and summarized our western blotting, qPCR, and morphometrical data in relation to wound age estimation (Table 3). Obviously, combination of multiple techniques and biomarkers suggests a more reliable wound age estimation. For example, the wound age was highly suggested to be approximately 3 days if (1) the average number of Pax7 + cells was between 20 and 35, the average numbers of MyoD + and myogenin + cells were > 50, regenerated myotubes were absent, and the ratio of myogenin + to Pax7 + cells in number was > 3.88; (2) the relative quantities of *Myod1*, *Myog*, and *Igf1* mRNA were > 2.78, > 7.80, and > 3.13, respectively. Likewise, we could also generally estimate the wound age of 7 days if the following conditions were met: (1) the average number of Pax7 + cells was between 20 and 35, the average number of myogenin$^+$ cells was > 50, and regenerated myotubes were present; (2) the relative quantities of MyoD, myogenin, and IGF-1 protein were > 1.40, > 1.57, and > 0.92, respectively; (3) the relative quantity of *Pax7* mRNA was > 2.44.

It is well-known that the process of wound healing in mammals, including rats, mice, and rabbits, is very similar to human. Animal experiments have the advantages of being well-controlled and standardized, which facilitate investigation of the wound healing process, including wound age estimation [5, 12]. A reproducible muscle contusion model of rats was applied for investigating wound age in our study, which provided valuable experimental data for skeletal muscle wound age estimation. However, a variety of factors, including individual variation, degree of damage, and postmortem interval, should be taken into account for wound age estimation in forensic practice [5, 12]. Thus, it is firstly required to perform further study by using human skeletal muscle specimens with a variety of wound ages in order to validate the applicability of these results to forensic practices.

In summary, from the perspective of morphometrics, mRNA expression, and protein expression, we demonstrated that Pax7, MyoD, myogenin, and IGF-1 expression levels were upregulated in a time-dependent manner during skeletal muscle wound healing in rats. This suggests the potential of these SC fate-related biomarkers as candidate indicators for wound age estimation in skeletal muscle contusion.

Funding The study was financially supported by grants from the National Natural Science Foundation of China (82171872), Natural Science Foundation of Shanghai (21ZR1464600), Shanghai Key Laboratory of Forensic Medicine (21DZ2270800), Shanghai Forensic Service Platform (19DZ2290900), and Central Research Institute Public Project (GY2020Z-4, GY2020G-4, GY2021G-4, GY2021G-5, and GY2022G-3).

Data availability The data generated and analyzed during the study are available from the corresponding authors on reasonable request.

Declarations

Ethical approval This article does not contain studies with human participants performed by any of the authors. The study complies with current ethical considerations for animals and was approved by the Academic Committee of China Medical University and Academy of Forensic Science (Ministry of Justice), People's Republic of China.

Consent to participate Not applicable.

Conflict of interest The authors declare no competing interests.

References

1. Kondo T (2007) Timing of skin wounds. Leg Med (Tokyo) 9:109–114
2. Wang LL, Zhao R, Liu CS, Liu M, Li SS, Li JY, Jiang SK, Zhang M, Tian ZL, Wang M, Zhang MZ, Guan DW (2016) A fundamental study on the dynamics of multiple biomarkers in mouse excisional wounds for wound age estimation. J Forensic Leg Med 39:138–146
3. Gaballah MH, Fukuta M, Maeno Y, Seko-Nakamura Y, Monma-Ohtaki J, Shibata Y, Kato H, Aoki Y, Takamiya M (2016) Simultaneous time course analysis of multiple markers based on DNA microarray in incised wound in skeletal muscle for wound aging. Forensic Sci Int 266:357–368
4. Kondo T, Ishida Y (2010) Molecular pathology of wound healing. Forensic Sci Int 203:93–98
5. Kondo T, Ohshima T (1996) The dynamics of inflammatory cytokines in the healing process of mouse skin wound: a preliminary study for possible wound age determination. Int J Legal Med 108:231–236
6. Kondo T, Tanaka J, Ishida Y, Mori R, Takayasu T, Ohshima T (2002) Ubiquitin expression in skin wounds and its application to forensic wound age determination. Int J Legal Med 116:267–272
7. Ohshima T (2000) Forensic wound examination. Forensic Sci Int 113:153–164
8. Takamiya M, Kumagai R, Nakayashiki N, Aoki Y (2006) A study on mRNA expressions of fibronectin in dermal and cerebral wound healing for wound age estimation. Leg Med (Tokyo) 8:214–219
9. Yu TS, Cheng ZH, Li LQ, Zhao R, Fan YY, Du Y, Ma WX, Guan DW (2010) The cannabinoid receptor type 2 is time-dependently expressed during skeletal muscle wound healing in rats. Int J Legal Med 124:397–404
10. Casse J-M, Martrille L, Vignaud J-M, Gauchotte G (2016) Skin wounds vitality markers in forensic pathology: an updated review. Med Sci Law 56:128–137
11. Ishida Y, Kimura A, Nosaka M, Kuninaka Y, Shimada E, Yamamoto H, Nishiyama K, Inaka S, Takayasu T, Eisenmenger W, Kondo T (2015) Detection of endothelial progenitor cells in human skin wounds and its application for wound age determination. Int J Legal Med 129:1049–1054
12. Li N, Du Q, Bai R, Sun J (2020) Vitality and wound-age estimation in forensic pathology: review and future prospects. Forensic Sci Res 5:15–24
13. Ma WX, Yu TS, Fan YY, Zhang ST, Ren P, Wang SB, Zhao R, Pi JB, Guan DW (2011) Time-dependent expression and distribution of monoacylglycerol lipase during the skin-incised wound healing in mice. Int J Legal Med 125:549–558

14. Sun JH, Zhu XY, Dong TN, Zhang XH, Liu QQ, Li SQ, Du QX (2017) An "up, no change, or down" system: time-dependent expression of mRNAs in contused skeletal muscle of rats used for wound age estimation. Forensic Sci Int 272:104–110
15. Tian ZL, Jiang SK, Zhang M, Wang M, Li JY, Zhao R, Wang LL, Li SS, Liu M, Zhang MZ, Guan DW (2016) Detection of satellite cells during skeletal muscle wound healing in rats: time-dependent expressions of Pax7 and MyoD in relation to wound age. Int J Legal Med 130:163–172
16. Järvinen TA, Järvinen TL, Kääriäinen M, Kalimo H, Järvinen M (2005) Muscle injuries: biology and treatment. Am J Sports Med 33:745–764
17. Karalaki M, Fili S, Philippou A, Koutsilieris M (2009) Muscle regeneration: cellular and molecular events. In Vivo 23:779–796
18. Relaix F, Zammit PS (2012) Satellite cells are essential for skeletal muscle regeneration: the cell on the edge returns centre stage. Development 139:2845–2856
19. Yin H, Price F, Rudnicki MA (2013) Satellite cells and the muscle stem cell niche. Physiol Rev 93:23–67
20. Powell DJ, McFarland DC, Cowieson AJ, Muir WI, Velleman SG (2014) The effect of nutritional status on myogenic gene expression of satellite cells derived from different muscle types. Poult Sci 93:2278–2288
21. Wang YX, Rudnicki MA (2012) Satellite cells, the engines of muscle repair. Nat Rev Mol Cell Biol 13:127–133
22. Diao Y, Guo X, Li Y, Sun K, Lu L, Jiang L, Fu X, Zhu H, Sun H, Wang H, Wu Z (2012) Pax3/7BP is a Pax7-and Pax3-binding protein that regulates the proliferation of muscle precursor cells by an epigenetic mechanism. Cell Stem Cell 11:231–241
23. Holterman CE, Rudnicki MA (2005) Molecular regulation of satellite cell function. Semin Cell Dev Biol 16:575–584
24. Legerlotz K, Smith HK (2008) Role of MyoD in denervated, disused, and exercised muscle. Muscle Nerve 38:1087–1100
25. Motohashi N, Asakura A (2014) Muscle satellite cell heterogeneity and self-renewal. Front Cell Dev Biol 2:1
26. Ogura Y, Mishra V, Hindi SM, Kuang S, Kumar A (2013) Proinflammatory cytokine tumor necrosis factor (TNF)-like weak inducer of apoptosis (TWEAK) suppresses satellite cell self-renewal through inversely modulating Notch and NF-κB signaling pathways. J Biol Chem 288:35159–35169
27. Mourkioti F, Rosenthal N (2005) IGF-1, inflammation and stem cells: interactions during muscle regeneration. Trends Immunol 26:535–542
28. Cecchi R (2010) Estimating wound age: looking into the future. Int J Legal Med 124:523–536
29. Tian ZL, Jiang SK, Zhang M, Wang M, Li JY, Zhao R, Wang LL, Liu M, Li SS, Zhang MZ, Guan DW (2015) α7nAChR is expressed in satellite cells at different myogenic status during skeletal muscle wound healing in rats. J Mol Histol 46:499–509
30. von Maltzahn J, Jones AE, Parks RJ, Rudnicki MA (2013) Pax7 is critical for the normal function of satellite cells in adult skeletal muscle. Proc Natl Acad Sci U S A 110:16474–16479
31. Hatade T, Takeuchi K, Fujita N, Arakawa T, Miki A (2014) Effect of heat stress soon after muscle injury on the expression of MyoD and myogenin during regeneration process. J Musculoskelet Neuronal Interact 14:325–333
32. Jennische E, Hansson HA (1987) Regenerating skeletal muscle cells express insulin-like growth factor I. Acta Physiol Scand 130:327–332
33. Philippou A, Barton ER (2014) Optimizing IGF-I for skeletal muscle therapeutics. Growth Horm IGF Res 24:157–163
34. Song Y-H, Song JL, Delafontaine P, Godard MP (2013) The therapeutic potential of IGF-I in skeletal muscle repair. Trends Endocrinol Metab 24:310–319
35. Fan YY, Zhang ST, Yu LS, Ye GH, Lin KZ, Wu SZ, Dong MW, Han JG, Feng XP, Li XB (2014) The time-dependent expression of α7nAChR during skeletal muscle wound healing in rats. Int J Legal Med 128:779–786
36. Ishida Y, Kimura A, Nosaka M, Kuninaka Y, Takayasu T, Eisenmenger W, Kondo T (2012) Immunohistochemical analysis on cyclooxygenase-2 for wound age determination. Int J Legal Med 126:435–440
37. Ishida Y, Kuninaka Y, Furukawa F, Kimura A, Nosaka M, Fukami M, Yamamoto H, Kato T, Shimada E, Hata S, Takayasu T, Eisenmenger W, Kondo T (2018) Immunohistochemical analysis on aquaporin-1 and aquaporin-3 in skin wounds from the aspects of wound age determination. Int J Legal Med 132:237–242
38. Ishida Y, Kuninaka Y, Nosaka M, Kimura A, Kawaguchi T, Hama M, Sakamoto S, Shinozaki K, Eisenmenger W, Kondo T (2015) Immunohistochemical analysis on MMP-2 and MMP-9 for wound age determination. Int J Legal Med 129:1043–1048
39. Kondo T, Ohshima T, Eisenmenger W (1999) Immunohistochemical and morphometrical study on the temporal expression of interleukin-1α (IL-1α) in human skin wounds for forensic wound age determination. Int J Legal Med 112:249–252
40. Kondo T, Ohshima T, Mori R, Guan DW, Ohshima K, Eisenmenger W (2002) Immunohistochemical detection of chemokines in human skin wounds and its application to wound age determination. Int J Legal Med 116:87–91
41. Abd-Elhakim YM, Omran BHF, Ezzeldein SA, Ahmed AI, El-Sharkawy NI, Mohamed AA (2022) Time-dependent expression of high-mobility group box-1 and toll-like receptors proteins as potential determinants of skin wound age in rats: forensic implication. Int J Legal Med 136(6):1781–1789. https://doi.org/10.1007/s00414-022-02788-z
42. Du QX, Sun JH, Zhang LY, Liang XH, Guo XJ, Gao CR, Wang YY (2013) Time-dependent expression of SNAT2 mRNA in the contused skeletal muscle of rats: a possible marker for wound age estimation. Forensic Sci Med Pathol 9:528–533
43. Fan YY, Ye GH, Lin KZ, Yu LS, Wu SZ, Dong MW, Han JG, Feng XP, Li XB (2013) Time-dependent expression and distribution of Egr-1 during skeletal muscle wound healing in rats. J Mol Histol 44:75–81

Authors and Affiliations

Zhi-Ling Tian[1] · Ruo-Lin Wang[2,3] · Qi-Fan Yang[1] · Zhi-Qiang Qin[1] · He-Wen Dong[1] · Dong-Hua Zou[1] · Zheng-Dong Li[1] · Jin-Ming Wang[1] · Da-Wei Guan[4] · Jian-Hua Zhang[1] · Ning-Guo Liu[1]

Zhi-Ling Tian
tzl201220166@163.com

Ruo-Lin Wang
ruolin101@163.com

[1] Shanghai Key Laboratory of Forensic Medicine, Shanghai Forensic Service Platform, Academy of Forensic Science, Ministry of Justice, 1347# West Guangfu Road, Shanghai 200063, People's Republic of China

[2] Zhe Jiang Di'an Institute of Forensic Science, Hangzhou 31000, People's Republic of China

[3] Shanghai Di'an Forensic Sciences Co., Ltd, Shanghai 200439, People's Republic of China

[4] Department of Forensic Pathology, China Medical University School of Forensic Medicine, 77# Puhe Road, Shenbei New District, Shenyang 110122, Liaoning Province, People's Republic of China